Rotational properties in even-even superheavy $^{254-258}$Rf nuclei based on total-Routhian-surface calculations*

WANG Hua-Lei(王华磊)[1;1)] CHAI Qing-Zhen(柴清祯)[1] JIANG Jin-Ge(蒋金鸽)[1] LIU Min-Liang(柳敏良)[2]

[1] School of Physics and Engineering, Zhengzhou University, Zhengzhou 450001, China
[2] Institute of Modern Physics, Chinese Academy of Sciences, Lanzhou 730000, China

Abstract: High-spin yrast structures of even-even superheavy nuclei $^{254-258}$Rf are investigated by means of total-Routhian-surface approach in three-dimensional (β_2, γ, β_4) space. The behavior in the moments of inertia of ^{256}Rf is well reproduced by our calculations, which is attributed to the $j_{15/2}$ neutron rotation-alignment. The competition between the rotationally aligned $i_{13/2}$ proton and $j_{15/2}$ neutron may occur to a large extent in ^{256}Rf. High-spin predictions are also made for its neighboring isotopes ^{254,258}Rf, showing that the alignment of the $j_{15/2}$ neutron pair is more favored than that of the $i_{13/2}$ proton pair.

Key words: rotational property, total-Routhian-surface calculation, moment of inertia, band crossing

PACS: 21.60.Ev, 21.10.Re, 27.90.+b **DOI:** 10.1088/1674-1137/38/7/074101

1 Introduction

Both experimentally and theoretically, the study of superheavy nuclei with $Z\gtrsim104$ is a fast developing area of nuclear physics [1, 2]. These nuclei are stabilized by a shell-correction energy, which originates from the rearrangement of single-particle orbitals and the occurrence of regions of low level density. The structures and formation mechanisms of shell-stabilized nuclei are governed by similar physics, which is responsible for the predicted stability of an island of superheavy nuclei around $Z=114$, $N=184$ (also $Z=120$, 124, or 126, depending on theoretical models and the parametrization employed) [3–5]. The precise location of the proposed new magic numbers depends sensitivity on the single-particle structure. Presently, the related single-particle levels of the new spherical shell cannot be directly investigated through either in-beam or decay spectroscopy because the production cross sections of these nuclei with $Z\geqslant110$ are very small.

However, a great number of spectroscopy measurements have been carried out to study yrast and non-yrast level structures, including high-K isomers, for the deformed nuclei of the transfermium mass region, typically with $Z\approx100$, $N\approx150-160$ [6–8]. High-spin rotational bands have been observed in many of them (e.g. $^{247,249}_{96}$Cm [9], $^{248,249,250,252}_{98}$Cf [9, 10], $^{250}_{100}$Fm [11], $^{251}_{101}$Md [12], $^{252,253,254}_{102}$No [13–16], $^{255}_{103}$Lr [17]). Theoretically, the nuclear properties of the transfermium nuclei have been systematically investigated using various methods, such as the macroscopic-microscopic models and the self-consistent mean-field models (see Refs. [4, 5, 18–20] and references therein). Although these nuclei are not really superheavy nuclei, they are at the gateway to the superheavy mass region. In particular, their high-spin information can provide an indirect way to study the single-particle states of the next spherical shell above $^{208}_{82}$Pb$_{126}$ because some of them are strongly down-sloping and thus can come close to the Fermi surface in the deformed region [21]. Moreover, these high-spin states also may give information on the fission barrier at high angular momentum, which is important for our understanding of the mechanism for producing the heaviest elements [13].

For the superheavy isotopes, spectroscopic studies are in a preliminary stage and detailed information on high-spin properties is still scarce [22]. Nevertheless, the ground-state band in the $Z=104$ isotope $^{256}_{104}$Rf$_{152}$, the first even-even superheavy element for which high-spin data now exist, was recently reported by Greenlees et al. [23]. Soon afterwards, the kinematic and dynamic moments of inertia of the ground-state band in $^{256}_{104}$Rf$_{152}$ was studied by using a particle-number conserving method that was based on a cranked shell model [24]. It is conceivable that with the help of the new generation detector systems and radioactive beam facilities [25, 26], the experimental spectroscopic borders of this region will

Received 30 August 2013

∗ Supported by National Natural Science Foundation of China (10805040, 11175217), Foundation and Advanced Technology Research Program of Henan Province (132300410125), S & T Research Key Program of Henan Province Education Department (13A140667)

1) E-mail: wanghualei@zzu.edu.cn

soon be expanded towards even heavier nuclei. In the present work, we aim to understand the high-spin states in the nucleus ^{256}Rf using self-consistent total-Routhian-surface (TRS) approach based on Woods-Saxon (WS) potential and predict the rotational behaviors of its neighboring even-even isotopes ^{254,258}Rf. Part of the aim of this work is to test the predictive power of the present model in superheavy nuclei. Although it is generally successful in other mass regions, different polarization effects and functional forms of the densities may occur in superheavy region. These effects can be naturally incorporated within the self-consistent nuclear mean-field models, but the preconceived knowledge about the expected densities and single-particle potentials, which fades away towards superheavy region, is required in the macroscopic-microscopic investigations [4].

2 The model

The TRS approach [27–29], which is based on the cranked shell model [30, 31], accounts well for the overall systematics of high-spin phenomena in rapidly rotating medium and heavy mass nuclei. The total Routhian, which is called "Routhian" rather than "energy" in a rotating frame of reference, is the sum of the energy of the non-rotating state and the contribution due to cranking. The energy of the non-rotating state consists of a macroscopic part that is obtained from the standard liquid-drop model [32] and a microscopic term representing the Strutinsky shell correction [33]. Single-particle energies needed in the calculation of the quantal shell correction are obtained from a triaxial WS potential [34, 35] with the parameter set widely used for cranking calculations. During the diagonalization process of the WS Hamiltonian, the oscillator states with the principal quantum number $N \leqslant 12$ and 14 have been used as a basis for protons and neutrons, respectively. The nuclear shape is defined by the standard parametrization in which it is expanded in spherical harmonics [35]. The deformation parameters include β_2, γ, and β_4 where γ describes nonaxial shapes. The pairing correlation is treated using the Lipkin-Nogami approach [36], in which the particle number is conserved approximately. This avoids the spurious pairing phase transition encountered in the simpler BCS calculation. Both monopole and doubly stretched quadrupole pairings are considered. The quadrupole pairing is important for the proper description of the moments of inertia, although it has a negligible effect on energies [37]. The monopole pairing strength, G, is determined by the average gap method [38] and the quadrupole pairing strengths are obtained by restoring the Galilean invariance broken by the seniority pairing force [29, 39]. The 80 single-particle levels, the respective 40 states just below and above the Fermi energy, are included in the pairing windows for both protons and neutrons. The Strutinsky quantal shell correction is performed with a smoothing range $\gamma=1.20\hbar\omega_0$, where $\hbar\omega_0=41/A^{1/3}$ MeV, and a correction polynomial of order $p=6$.

The nuclear system is cranked around a fixed axis (the x-axis) at a given rotational frequency ω. Pairing correlations are dependent on rotational frequency and deformation. The resulting cranked-Lipkin-Nogami equation takes the form of the well known Hartree-Fock-Bogolyubov-like (HFB) equation [29]. For a given rotational frequency and point of deformation lattice, the pairing is treated self-consistently by solving this equation using a sufficiently large space of WS single-particle states. Certainly, symmetries of the rotating potential can be used to simplify the cranking equations. In the reflection-symmetric case, both signature, r, and intrinsic parity, π are good quantum numbers. The solution characterized by (π, r) simultaneously provides the energy eigenvalue, from which it is straightforward to obtain the energy relative to the non-rotating state. After the numerical calculated Routhians at fixed ω are interpolated using cubic spline function between the lattice points, the equilibrium deformation can be determined by minimizing the calculated TRS. The absolute minimum of the TRS corresponds to the solution for a yrast state. Secondary ones correspond to other solutions, which may be yrast at higher spins.

3 Results and discussions

To test the validity of current nuclear potential, single-particle levels calculated for $^{256}_{104}\mathrm{Rf}_{152}$ are shown in Fig. 1 for protons and neutrons, respectively. The typical spherical and deformed shell gaps can clearly be seen, which indicate the best candidates for spherical and deformed nuclei. For example, the combination of the $Z=108$ and $N=162$ gaps at $\beta_2\approx0.24$ leads to $^{270}_{108}\mathrm{Hs}_{162}$, which was predicted to be doubly magic deformed nucleus [40]. The effect of the known deformed shell at the neutron number N=152 is also reproduced in the results for the mass region. The properties of the single-particle structures are in good agreement with the previous study by Sobiczewski et al. [41]. The present results are also supported by the microscopic corrections calculated by Möller et al. [42], which are related to single-particle level density (low level density results in a large correction energy). In Fig. 1, the unique-parity high-j intruder orbitals are $1i_{13/2}$ proton and $1j_{15/2}$ neutron orbitals. The proton (neutron) Fermi surface is just above $\pi1/2^-[521]$ ($\nu9/2^-[734]$) orbital, which is filled in Z=103 and 104 (N=151 and 152) nuclei. As known, the study of odd-A nuclei can provide important information on single-particle structures. In the present calculation,

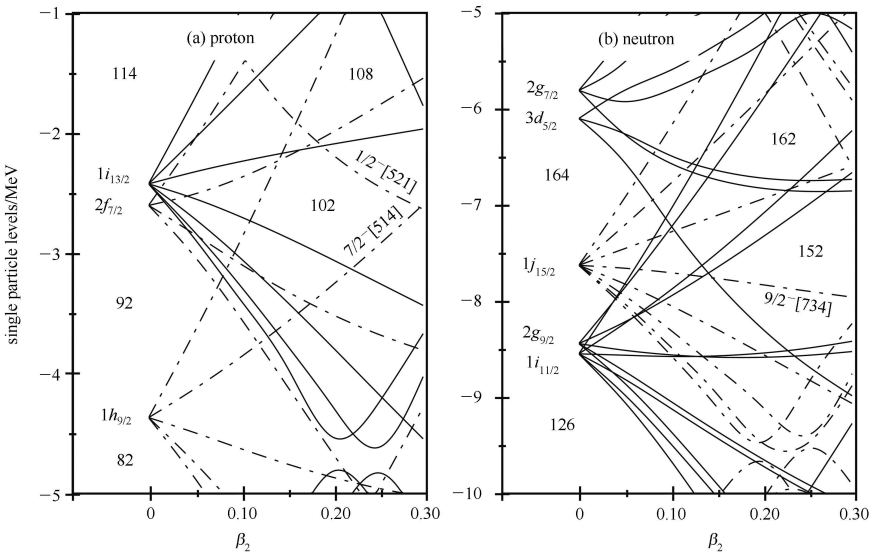

Fig. 1. The calculated Woods-Saxon single particle levels near the Fermi surface of $^{256}_{104}\mathrm{Rf}_{152}$ (a) for protons and (b) for neutrons. The positive (negative) parity levels are denoted by the solid (dot-dash) lines.

the sequence of single-proton levels near the Fermi surface is quite similar to that determined from the experimental information of $^{255}_{103}\mathrm{Lr}_{152}$ isotone [43], in which the energies of $1/2^-[521](2f_{5/2})$ and $7/2^-[514](1h_{9/2})$ are nearly degenerate. In $^{255}_{104}\mathrm{Rf}_{151}$ isotope [44], the ground-state configuration is suggested to be $9/2^-[734](1j_{15/2})$ by experiment, which is also consistent with our calculation.

In principle, the study of multi-quasiparticle excitations can be used to determine the excitation energies and ordering of the single-particle states near the Fermi surface. For example, two 2-quasiproton isomeric states are reported in ^{254}No by Herzberg et al. [45], one with a K-value and parity of $K^\pi=8^-(9/2^+[624]\otimes 7/2^-[514])$ and the other with a $K^\pi=3^+(1/2^-[521]\otimes 7/2^-[514])$. The excitation energies of the 3^+ and 8^- states were found at 0.988 and 1.296 MeV, which indicates that the single-particle energy of $1/2^-[521]$ orbital is lower than that of the $9/2^+[624]$ orbital. Similarly, 2-quasiparticle isomeric states in ^{256}Rf are expected to be identified, which can provide a test for current nuclear model. Experiments on quasiparticle excitations for ^{256}Rf have been performed by Jeppesen et al. [46] and by Robinson et al. [47]. However, the search for the 2-quasiparticle states has not been very successful, even their experimental results and interpretation are in disagreement and conflict. Up to now, there is no convincing evidence for the existence of 2-quasiparticle states in ^{256}Rf, thus additional experimental investigation is highly desirable.

The present TRS calculations based on the WS potential are performed in the lattice of quadrupole (β_2, γ) deformations with hexadecapole (β_4) variation. Since our previous investigation [48], the inclusion of reflection-asymmetric deformation degrees of freedom shows that there is no octupole instabilities at normal deformed minima for the lighter Rf isotopes. In Fig. 2, the evolutions of calculated β_2, β_4 and γ deformations with increasing rotational frequency are displayed for the even-even $^{254-258}$Rf nuclei studied here. These nuclei are predicted to have well-deformed prolate shapes with very small γ deformation. Note that the calculated ground-state β_2 deformations, typically ≈ 0.24, are basically consistent with the previous results given by Möller et al. [42] and by Sobiczewski et al. [41]. The associated β_2 deformations are rather stable and decrease slightly with increasing rotational frequency. In our opinion, the decrease of β_2 as a function of rotational frequency is due to the mixing between the g-band and a 2-quasiparticle ($\pi i_{13/2}$ or $\nu j_{15/2}$ quasi-particles) aligned band. It seems that a rapid decrease of β_2 appears after a critical frequency $\approx$0.3 MeV, which indicates the band crossing frequency. For prolate deformed nuclei, the rotation-induced deoccupation of the antialigned high-j low-Ω quasiparticle orbitals can cause the nucleus to become less deformed [49]. The $\pi i_{13/2}$ alignment and the $\nu j_{15/2}$ alignment seem to produce slightly triaxial shapes.

Figure 3 shows the kinematic and dynamic moments of inertia, $J^{(1)}$ ($J^{(1)}=\hbar^2(2I-1)/E_\gamma(I)$) and $J^{(2)}$ ($J^{(2)}=4\hbar^2/[E_\gamma(I)-E_\gamma(I-2)]$), for the ground-state bands of even-even nuclei $^{254-258}$Rf, which can usually provide useful information on the energies of single-particle orbitals, particularly of those with high j. The level spins adopted here are obtained from Ref. [23], which are further confirmed by Zhang et al. [24]. One can see that the agreement of the moments of inertia for ^{256}Rf between theory and experiment is to a great extent excellent. The

moments of inertia $J^{(1)}$, $J^{(2)}$ show a gradual increase, reflecting a large-interaction band crossing, and essentially no difference among even-even $^{254-258}$Rf nuclei, especially at low frequencies. The upbending phenomena due to the alignment of $j_{15/2}$ neutrons and $i_{13/2}$ protons are clearly seen in Fig. 3. In general, the changes in the moments of inertia can be well understood in terms of the changing deformations or/and pairing correlations. The quadrupole deformation β_2 usually has an important effect on the moments of inertia. However, from the ω dependences of β_2 in Fig. 2, we observe a nearly constant behavior for the low-spin region and a sudden decrease in the high-spin states where rotation-alignment occurs. Obviously, the increase in moment of inertia, as shown in Fig. 3, cannot be explained by an increasing deformation β_2. It should instead be attributed to a decrease in the nucleon pairing correlations due to the Coriolis anti-pairing (CAP) effect. The slightly negative γ deformation may result in a change in the moment of inertia.

To understand the changing properties in the moments of inertia, we display the calculated collective angular momenta for even-even $^{254-258}$Rf nuclei in Fig. 4, together with proton and neutron components. As expected, the aligned angular momentum shows a similar changing trend to the moment of inertia (note that its slope means the moment of inertia $J^{(2)}$). It can be seen that a substantial increase of the total aligned angular momentum is due to the neutron contribution, although both proton and neutron components increase gently with increasing frequency. A sudden rise in the aligned angular momentum indicates an additional contribution from the rotation-alignment of a pair of high-j nucleons. In this mass region, the related high-j single-particle states are proton $i_{13/2}$ and neutron $j_{15/2}$ orbitals. About 30 years ago, the alignment properties of these orbitals in the actinides were surveyed by Frauendorf et al. [31, 50] and by Simon et al. [51, 52]. Moreover, the behaviour of the simultaneous alignment of protons and neutrons has been noticed in different nuclei such as in ^{235}U and ^{237}Np [31]. Recently, several studies [5, 20, 53]

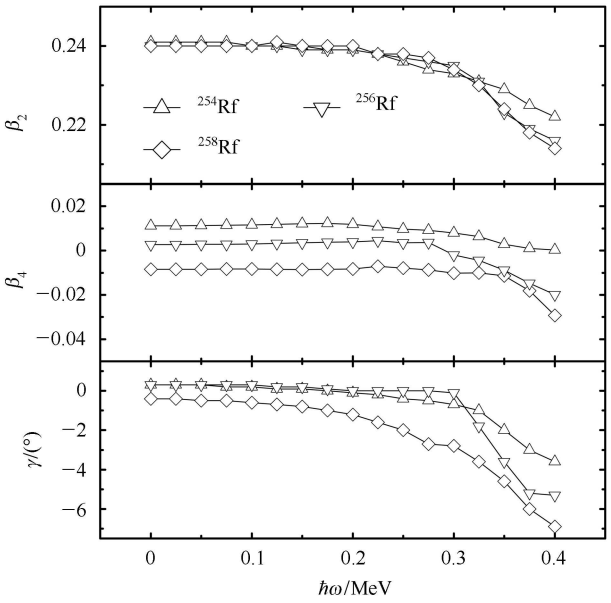

Fig. 2. The calculated deformations β_2 (top), β_4 (middle) and γ (bottom) versus the rotational frequency $\hbar\omega$ for even-even nuclei $^{254-258}$Rf.

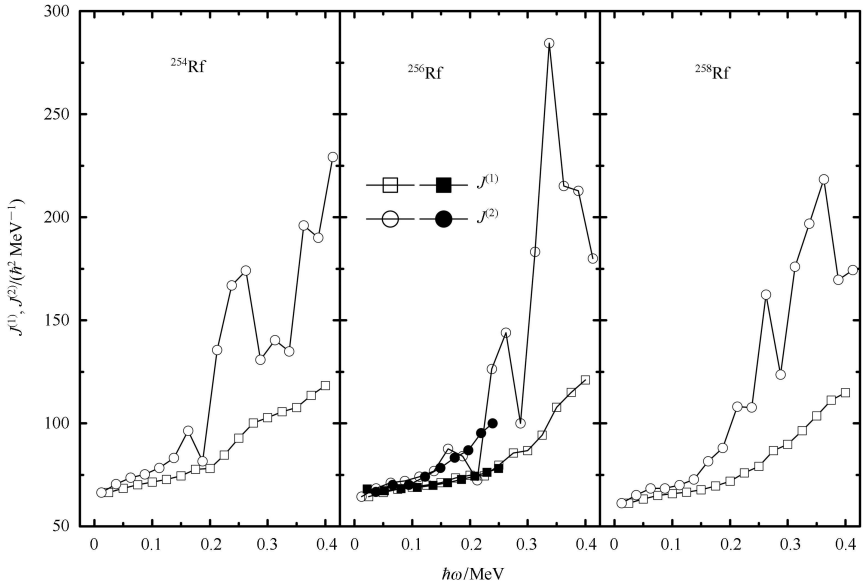

Fig. 3. The kinematic and dynamic moments of inertia $J^{(1)}$ and $J^{(2)}$ of even-even nuclei $^{254-258}$Rf versus the rotational frequency $\hbar\omega$ from experiments (filled symbols) and present calculations (open symbols). The experimental data are taken from Ref. [23].

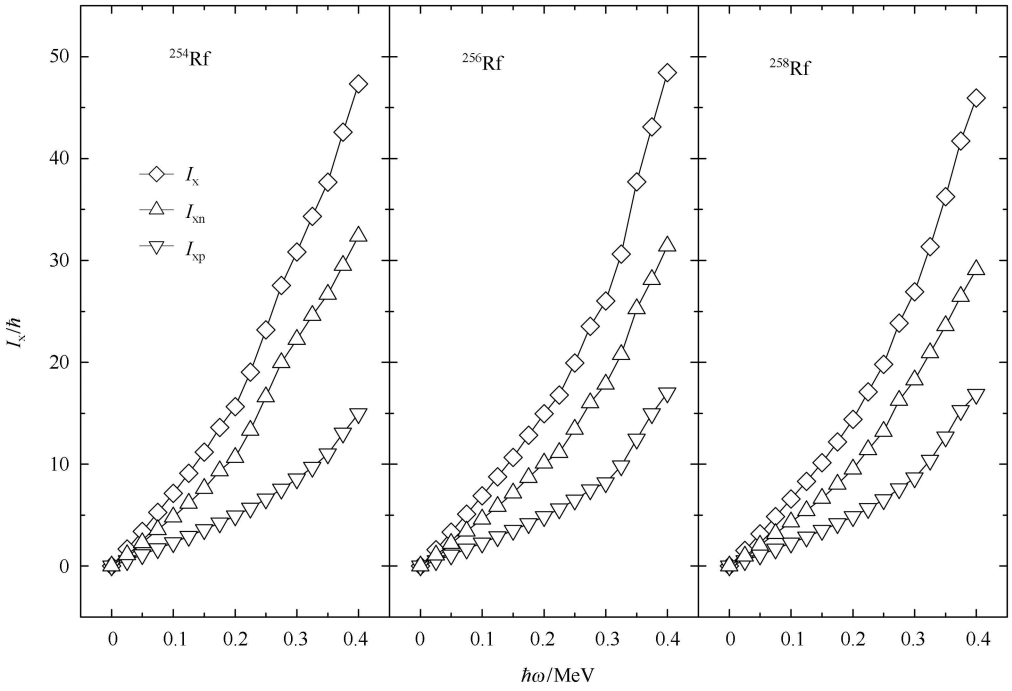

Fig. 4. The calculated aligned angular momentum as a function of rotational frequency $\hbar\omega$ for even-even nuclei $^{254-258}$Rf. Proton and neutron contributions are shown simultaneously.

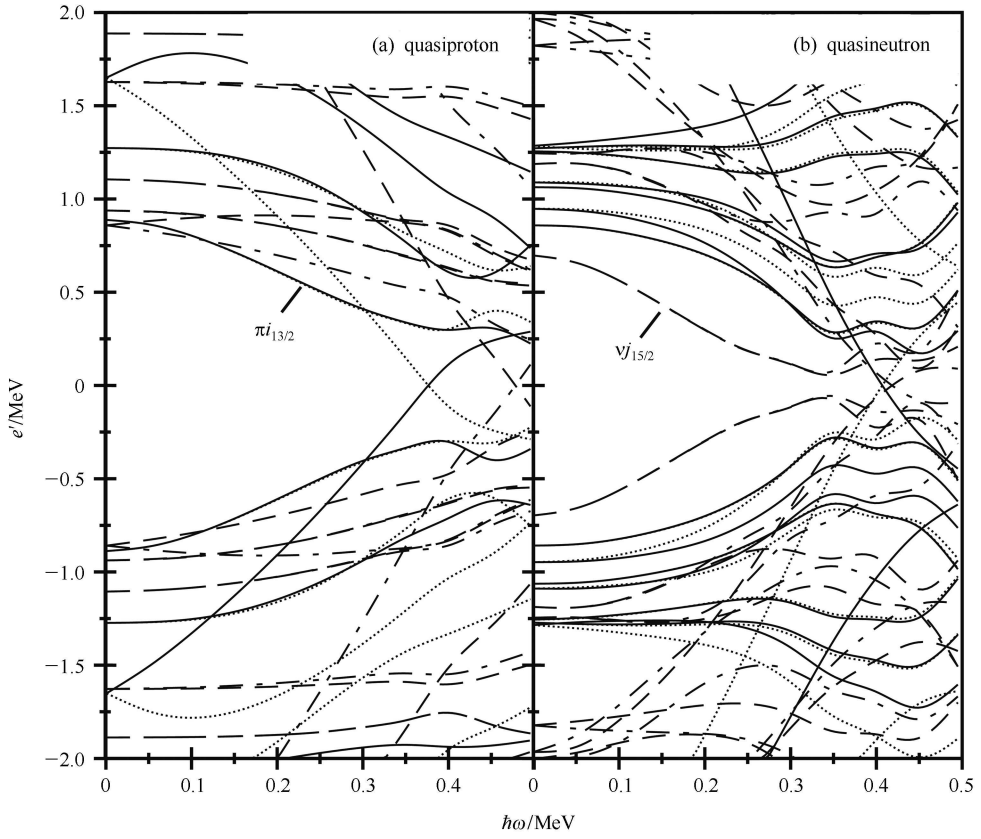

Fig. 5. The calculated quasiproton Routhians (a) and quasineutron Routhians (b) as functions of rotational frequency $\hbar\omega$. The deformation parameters used correspond to the yrast configurations of even-even nucleus ^{256}Rf. The parity and signature (π, α) of the Routhians are presented as follows: (+,+1/2) solid lines, (+,−1/2) dotted lines, (−,+1/2) dashed-dotted lines, and (−,−1/2) dashed lines.

have indicated that the alignments of $i_{13/2}$ proton and $j_{15/2}$ neutron pairs are also strongly competitive in some transfermium nuclei (heavy actinides). For example, it was pointed out that the proton and neutron alignments take place simultaneously in the lighter No isotopes (e.g. in ^{252,254}No), while the $j_{15/2}$ neutrons win in the competition between proton- and neutron-alignment in the heavier No isotopes (e.g. in ^{256,258}No) [20]. Fig. 4 shows that the first band crossing is most likely to be ascribed to the rotation-alignment of a pair of $j_{15/2}$ neutrons for the ^{254,258}Rf nuclei and there is a possible competition in rotation-alignment between high-j intruder protons and neutrons for ^{256}Rf because the proton and neutron up-bending frequencies seem to be somewhat close to each other.

The diagram of the quasi-particle Routhians versus rotational frequency is a convenient way to display the interplay between rotation and microscopic structure. By studying the quasi-particle diagram, as shown in Fig. 5, one can see the relevant quasi-particles are those from the unique-parity high-j intruder orbitals with $\pi i_{13/2}$ for protons and $\nu j_{15/2}$ for neutrons. The $\nu j_{15/2}$ band crossing in ^{256}Rf is calculated to occur slightly earlier than that for $\pi i_{13/2}$, which indicates a competitive behavior to some extent. In contrast, our calculation predicts that the alignment of the $1j_{15/2}$ neutron pair is more favored than the $\pi i_{13/2}$ alignment in ^{254,258}Rf. Moreover, similar to the situation in $N=152$ ^{254}No isotone [18], a delayed alignment is calculated to occur in ^{256}Rf.

4 Summary

In the present work, we have studied the evolution properties of the deformations and moments of inertia for even-even $^{254-258}$Rf nuclei by using self-consistent TRS method based on WS potential in (β_2, γ, β_4) deformation space. Our results are compared with previous calculations and available experiments. It is shown that the single-particle potential is still valid in the superheavy region and the deformed shell gaps (e.g. at $N=152$ and 162) are well reproduced. The calculated moments of inertia of ^{256}Rf are in good agreement with experiments and the up-bending is attributed to rotation-alignment of $1j_{15/2}$ neutron pair, showing a competitive property to some extent. Our prediction of rotational properties for ^{254,258}Rf awaits future experimental confirmation. It is clear, however, that high-spin experiments on ^{254,258}Rf, whose correction energies are smaller than that of the deformed magic number $N=152$ ^{256}Rf nucleus, will meet a great challenge due to the large fission probabilities.

References

1 Sobiczewski A, Pomorski K. Prog. Part. Nucl. Phys., 2007, **58**: 292
2 Schädel M. Angew. Chem., Int. Ed., 2006, **45**: 368
3 Nilsson S G et al. Nucl. Phys. A, 1968, **115**: 545
4 Rutz K et al. Phys. Rev. C, 1997, **56**: 238
5 ZHANG Z H et al. Phys. Rev. C, 2012, **85**: 014324
6 Herzberg R D. J. Phys. G, 2004, **30**: R123
7 Greenlees P T. Nucl. Phys. A, 2007, **787**: 507c
8 Eeckhaudt S et al. Eur. Phys. J. A, 2005, **26**: 27
9 Tandel S K et al. Phys. Rev. C, 2010, **82**: 041301(R)
10 Takahashi R et al. Phys. Rev. C, 2010, **81**: 057303
11 Bastin J E et al. Phys. Rev. C, 2006, **73**: 024308
12 Chatillon A et al. Phys. Rev. Lett., 2007, **98**: 132503
13 Reiter P et al. Phys. Rev. Lett., 1999, **82**: 509
14 Reiter P et al. Phys. Rev. Lett., 2005, **95**: 032501
15 Herzberg R D et al. Eur. Phys. J. A, 2009, **42**: 333
16 Herzberg R D et al. Phys. Rev. C, 2001, **65**: 014303
17 Ketelhut S et al. Phys. Rev. Lett., 2009, **102**: 212501
18 LIU H L, XU F R, Walker P M. Phys. Rev. C, 2012, **86**: 011301
19 ZHENG S J et al. Chin. Phys. C (HEP & NP), 2009, **33**: 107
20 Al-Khudair F, LONG G L, SUN Y. Phys. Rev. C, 2009, **79**: 034320
21 CHEN Y S, SUN Y, GAO Z C. Phys. Rev. C, 2008, **77**: 061305(R)
22 Berryman J S et al. J. Phys.: Conf. Ser., 2011, **312**: 092017
23 Greenlees P T et al. Phys. Rev. Lett., 2012, **109**: 012501
24 ZHANG Z H, MENG J, ZHAO E G, ZHOU S G. Phys. Rev. C, 2013, **87**: 054308
25 WANG H L et al. Chin. Phys. C (HEP & NP), 2010, **34**: 379
26 LIU W et al. Sci. Chin. Phys. Mech. Astron, 2011, **54**(Suppl.1): 14
27 Nazarewicz W, Leander G A, Dudek J. Nucl. Phys. A, 1987, **467**: 437
28 Satuła W, Wyss R, Magierski P. Nucl. Phys. A, 1994, **578**: 45
29 XU F R, Statuła W, Wyss R. Nucl. Phys. A, 2000, **669**: 119
30 Bengtsson R, Frauendorf S. Nucl. Phys. A, 1979, **327**: 139
31 Frauendorf S. Phys. Scr., 1981, **24**: 349
32 Myers W D, Swiatecki W J. Nucl. Phys. A, 1966, **81**: 1
33 Strutinsky V M. Nucl. Phys. A, 1967, **95**: 420
34 Nazarewicz W et al. Nucl. Phys. A, 1985, **435**: 397
35 Ćwiok S et al. Comput. Phys. Commun., 1987, **46**: 379
36 Pradhan H C, Nogami Y, Law J. Nucl. Phys. A, 1973, **201**: 357
37 Statuła W, Wyss R. Phys. Scr. T, 1995, **56**: 159
38 Möller P, Nix J R. Nucl. Phys. A, 1992, **536**: 20
39 Sakamoto H, Kishimoto T. Phys. Lett. B, 1990, **245**: 321
40 Patyk K, Sobiczewski A. Nucl. Phys. A, 1991, **533**: 132
41 Sobiczewski A, Muntian I, Patyk Z. Phys. Rev. C, 2001, **63**: 034306
42 Möller P, Nix J R. At. Data Nucl. Data Tables, 1995, **59**: 195
43 Chatillon A et al. Eur. Phys. J. A, 2006, **30**: 397
44 Heßberger F et al. Eur. Phys. J. A, 2006, **30**: 561
45 Herzberg R D et al. Nature(London), 2006, **442**: 896
46 Jeppesen H B et al. Phys. Rev. C, 2009, **79**: 031303(R)
47 Robinson A P et al. Phys. Rev. C, 2011, **83**: 064311
48 WANG H L, LIU H L, XU F R, JIAO C F. Chin. Sci. Bull., 2012, **57**: 1761
49 Petrache C M et al. Phys. Rev. C, 1998, **57**: R10
50 CHEN Y, Frauendorf S. Nucl. Phys. A, 1983, **393**: 135
51 Simon R S et al. Z. Phys. A, 1980, **298**: 121
52 Simon R S et al. Phys. Lett. B, 1982, **108**: 87
53 Afanasjev A V, Khoo T L, Frauendorf S. Phys. Rev. C, 2003, **67**: 024309